

Testing quantum theory with higher-order interference in many-particle correlations

Marc-Oliver Pleinert,^{1,2,3} Alfredo Rueda,^{1,4} Eric Lutz,⁵ and Joachim von Zanthier^{1,3}

¹*Institut für Optik, Information und Photonik,*

Friedrich-Alexander-Universität Erlangen-Nürnberg (FAU), 91058 Erlangen, Germany

²*International Max Planck Research School - Physics of Light (IMPRS-PL),*

Max Planck Institute for the Science of Light, 91058 Erlangen, Germany

³*Erlangen Graduate School in Advanced Optical Technologies (SAOT),*

Friedrich-Alexander-Universität Erlangen-Nürnberg (FAU), 91052 Erlangen, Germany

⁴*currently at: Scantinel Photonics, Carl-Zeiss-Strasse 22, 73447 Oberkochen, Germany*

⁵*Institute for Theoretical Physics I, University of Stuttgart, D-70550 Stuttgart, Germany*

Quantum theory permits interference between indistinguishable paths but, at the same time, restricts its order. Interference in single-particle correlations, for instance, is limited to the second order, that is, to pairs of single-particle paths. To date, all experimental efforts to search for higher-order interferences beyond those compatible with quantum mechanics have been based on such single-particle correlations. However, quantum physics is not bounded to interference in single-particle correlations. We here experimentally study higher-order interference in many-particle correlations using a two-photon-five-slit setup. We demonstrate that two-particle correlations exhibit nonzero interference up to the fourth order, corresponding to the interference of two distinct two-particle paths. We further show that fifth-order interference is restricted to 10^{-3} in the intensity-correlation regime and to 10^{-2} in the photon-correlation regime, thus providing novel bounds on the accuracy of quantum theory.

Interference phenomena for both light and matter are an intrinsic property of quantum physics. They occur when indistinguishable paths exist as in Young's paradigmatic double-slit experiment [1]. From a fundamental point of view, quantum interference stems from coherent superpositions of states and thus from the linearity of quantum theory [2]. However, quantum mechanics not only enables but also restricts interference [3]. For instance, according to Born's rule, which relates detection probabilities to the modulus square of the wave function [4], interference in single-particle correlations is limited to the second order, that is, to two interfering single-particle paths. In a multi-slit setup, interference is therefore expected to occur only between pairs of indistinguishable paths, and all higher orders in the interference hierarchy vanish [3]. In this case, the detection probability can be expressed as a sum of first-order and second-order terms.

The physical origin of the lack of higher-order quantum interferences is not yet understood [3]. Their existence would have profound implications for quantum theory, including nonlocality and contextuality [5–8]. They have indeed been linked to violations of the spatial [5] and temporal [6] Tsirelson bounds, as well as to a weakening of noncontextuality bounds [7]. They would hence reveal stronger-than-quantum correlations. They would further permit perfect interaction-free measurements [8]. For this reason, a growing number of single-particle experiments have been realized in the past years to detect such higher-order interference, using photons [9–12], molecules [13], atoms [14] and spin systems [15, 16].

Quantum physics, however, goes beyond interference in single-particle correlations. It also allows for many-particle interference in the case of indistinguishable particles. A prominent example is provided by the Hong-

Ou-Mandel experiment, in which two non-interacting photons can influence each other via two-particle interference [17]. Interference in many-particle correlations is mathematically richer and physically more subtle than single-particle interference [18–21]. It has found widespread applications in metrology [22, 23], imaging [24–26], and quantum information processing [27, 28]. Recently, the interference hierarchy has been theoretically extended to the general case of M -particle correlations with N modes [29]. In this situation, Born's rule allows for higher-order interference of up to the order $2M$. In addition, owing to the much larger number of interfering paths, many-particle interference has been predicted to offer increased sensitivity to deviations from quantum theory compared to its single-particle counterpart [29].

We here report the first experimental investigation of higher-order quantum interference in many-particle correlations using a two-photon-five-slit setup. We determine single-particle and two-particle interferences up to the fifth order, both in the intensity and in the photon-counting regimes. To this end, we measure and evaluate first-order and second-order correlation functions for a total of $2^5 = 32$ different interference configurations. While single-particle interference vanishes at the third order, we demonstrate that two-particle interference only cancels at the fifth order, in agreement with standard quantum theory.

Experimental setup. In order to assess single-particle and two-particle interference orders, we realize and analyze different experimental arrangements [Fig. 1(a)]: Photons, in a coherent state $|\alpha\rangle$ with mean photon number $\bar{n} = |\alpha|^2$, are provided by a HeNe laser at $\lambda = 633$ nm. These photons are scattered at two slit masks S1 and S2 [Figs. 1(b-c)]. The base slit mask S1 is a five-fold slit (denoted $ABCDE$), while the movable blocking slit mask

S2 consists of 33 configurations. Both masks have the same distance of adjacent slits $d = 500 \mu\text{m}$. By moving the blocking slit mask S2 in front of the fixed slit mask S1, we can implement all possible slit arrangements from one to five slits. For instance, in Fig. 1(a), slits A and E of S1 are blocked by S2 such that the three-slit configuration BCD is realized. The base mask S1 is fixed, reducing alignment errors. Moreover, we have added a second five-fold slit $ABCDE$ at the top of S2 to compare the interference patterns at the beginning and the end of a measurement sequence and thus verify the alignment of the setup. The measurement is conducted in the far-field at a distance $L = 1.7\text{m}$ behind the first slit mask either (i) in the intensity regime by a specialized, high-performance 14-bit charge-coupled device (CCD) camera [pco.pixelfly] or (ii) in the photon-counting regime by two fiber-coupled single-photon avalanche diodes (SPADs) [MPD PDM SPD-050-CTB-FC], whose signals are time-registered and correlated. The whole measurement process, including switching between different slit configurations and the data acquisition, is fully automatized to reduce errors further.

The measurement results can be interpreted in the few-particle regime by expanding the input photon state as

$$|\alpha\rangle = c_0 |0\rangle + c_1 |1\rangle + c_2 |2\rangle + \dots, \quad (1)$$

where $p_n = |c_n|^2$ is the Poissonian probability of the n -photon state to occur at the input. Whenever we register a photon in only one of the two SPADs, the effective input state is given by $|1\rangle$, which has been coherently distributed over the slits, leading to single-particle correlations. For a coincident detection at both detectors, the effective input state is $|2\rangle$, yielding two-particle correlations. Accordingly, we can measure both interference hierarchies simultaneously and differentiate between them by filtering the events via postselection.

Interference hierarchy. Many-particle correlations of noninteracting photons along indistinguishable M -particle paths are conveniently described by the M th-order intensity correlation function [30],

$$G^{(M)}(\delta_1, \dots, \delta_M) \propto \langle \hat{a}_1^\dagger \dots \hat{a}_M^\dagger \hat{a}_M \dots \hat{a}_1 \rangle, \quad (2)$$

where $\hat{a}_i \equiv \hat{a}(\delta_i)$ is the annihilation operator of the spatial mode $\delta_i = k d \sin \theta_i$, determined by the wave vector k , the slit distance d and the angle of the i th detector θ_i . Interference in such M -particle correlations can be classified into various orders $I_N^{(M)}$, depending on how many different modes (A, B, \dots) interfere with each other.

For single particles ($M = 1$), the first-order interference is trivially given by the (relative) detection probability in the far field, $I_1^{(1)} = P_A = G_A^{(1)}$, for a single slit A . The second-order interference is obtained by comparing the quantum-mechanical double-slit (AB) signal with the classical sum of the two single slits (A and B) [3],

$$I_2^{(1)} = G_{AB}^{(1)} - (G_A^{(1)} + G_B^{(1)}). \quad (3)$$

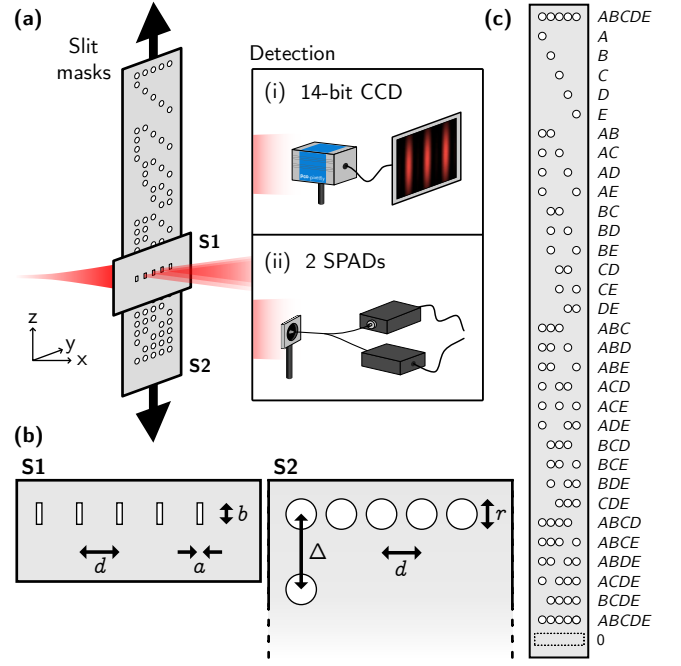


FIG. 1. **Setup to measure the interference hierarchy in single-particle and two-particle correlations.** (a) Coherent photons are sent through two slit masks, S1 and S2, and measured in the far field, either (i) by a charge coupled device (CCD) or (ii) by two single photon avalanche diodes (SPADs). (b) Fixed base slit mask S1 with dimensions $a = 25 \mu\text{m}$, $b = 200 \mu\text{m}$ and $d = 500 \mu\text{m}$. The dimensions of the movable slit mask S2 are $r = 400 \mu\text{m}$ with a spacing $\Delta = 1000 \mu\text{m}$. (c) The layout of slit mask S2 contains 33 configurations.

Higher orders can be constructed accordingly [3, 29] and the explicit expressions are given in Fig. 2. For single-particle correlations, all higher-order terms vanish, $I_3^{(1)} = I_4^{(1)} = I_5^{(1)} = \dots = 0$ [3]. The single-particle interference hierarchy hence truncates at the third order.

By contrast, for two particles ($M = 2$), nonzero interference occurs up to the fourth order [29],

$$I_2^{(2)} \neq 0, I_3^{(2)} \neq 0, I_4^{(2)} \neq 0; I_5^{(2)} = I_6^{(2)} = \dots = 0. \quad (4)$$

Born's rule hence allows for the interference of two two-particle paths, and the two-particle interference hierarchy is only truncated at the fifth order.

The vanishing of higher-order interference in many-particle correlations is captured by the M -particle Sorkin parameter defined as the normalized $(2M + 1)$ th interference [29],

$$\kappa^{(M)} = \frac{I_{2M+1}^{(M)}}{G_{A,B,C,\dots}^{(M)}(0,0,0,\dots)}, \quad (5)$$

where the first member ($M = 1$) is the single-particle Sorkin parameter [3]. According to quantum mechanics, Eq. (5) is zero for all M .

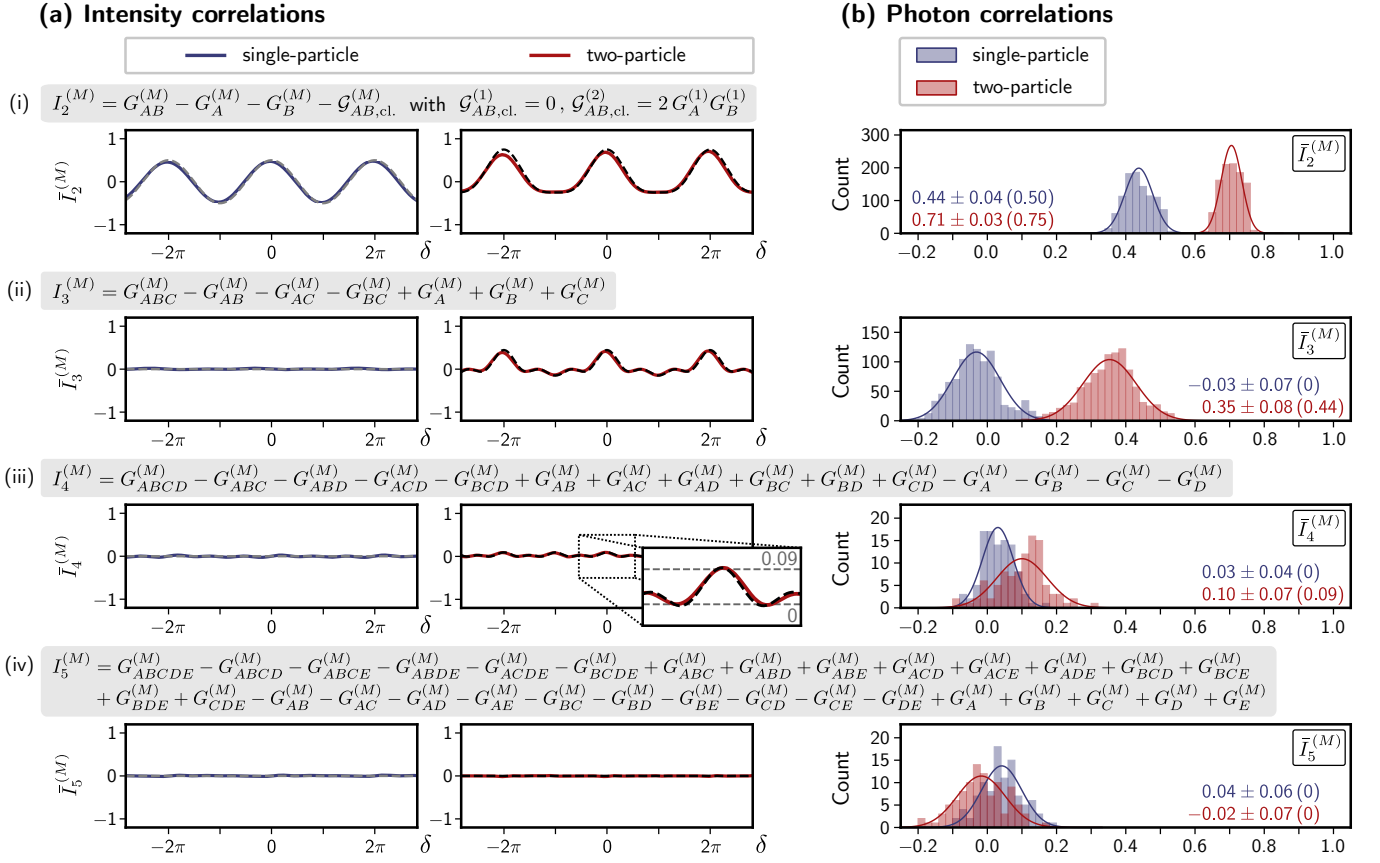


FIG. 2. **Experimental results of the interference hierarchy.** Interference orders in (a) the intensity-correlation regime and (b) the photon-correlation regime from (i) the second order to (iv) the fifth order (related formulas are taken from Ref. [29]). (a) Experimental data (solid) and quantum-mechanical theory (dashed) of single-particle (blue, left) and two-particle (red, right) interference orders. Fourth-order two-particle interference exhibits a tiny modulation, clearly visible with a good signal-to-noise ratio and most pronounced at the center (inset). (b) Histograms of the single-particle (blue) and two-particle (red) interference hierarchy at $\delta = 0$ in the photon-counting regime.

Experimental results. To obtain the complete interference hierarchy of single-particle and two-particle correlations, we perform 31+1+1 (correlation) measurements. The latter consist of the measurement of 31 different slit configurations needed to evaluate the interference orders, one additional measurement for the second $ABCDE$ arrangement added at the top of the slit mask S2, and one final measurement of the background (0), where the mask S2 blocks all slits of the base mask S1. These 33 measurements form a measurement set.

At the beginning of such a set, the measurement sequence is randomized to reduce systematic errors. A motorized translation stage addresses the slit mask S2 and implements the drawn slit configuration $X \in \{ABCDE(1), A, B, \dots, ABCDE(2), 0\}$. In the intensity regime, we take 250 CCD images of each slit configuration. The integration time $t_i = 2$ ms is fixed for all configurations and fully covers the CCD's dynamical range when measuring $ABCDE$. In the photon-counting regime, the two SPADs register the single-photon and two-photon events within a fixed total time of $T = 20$ s

per slit configuration. Time tags of the photon events are registered by a time-to-digital converter and correlated within a time frame of $t_f = 1$ ns. We ensure that the count rates are below 100 kHz such that detector nonlinearities can be neglected (with the dead time of the SPADs being 77 ns). We record the data in the autocorrelation scheme, where both detectors are effectively at the same position ($\delta_1 = \delta_2 = \delta$). This scheme is least sensitive to alignment errors. For intensity measurements, each pixel of the CCD can be regarded as an independent detector, and the autocorrelation function is measured by correlating pixels of the same optical phase δ from neighboring lines of the CCD. On the other hand, for photon-counting measurements, the autocorrelation is implemented by a fiber beam splitter at δ , connected to the two different SPADs.

In total, we perform 100 such measurement sets, each with a different sequence, in the intensity regime as well as in the photon-counting regime. For each set, the data is averaged per slit configuration and corrected by subtracting background and detector noise. From

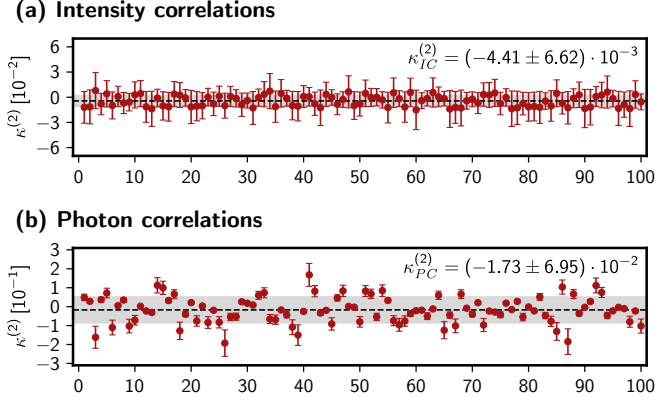


FIG. 3. **Two-particle Sorkin parameter.** Parameter $\kappa^{(2)}$ from Eq. (5) for 100 measurement sets in (a) the intensity-correlation regime and (b) the photon-correlation regime. In (b), the error bars are enlarged by a factor 100.

the corrected data, we evaluate the two-particle interference orders, $I_2^{(2)}, I_3^{(2)}, I_4^{(2)}, I_5^{(2)}$ as well as the single-particle interference orders, $I_2^{(1)}, I_3^{(1)}, I_4^{(1)}, I_5^{(1)}$, from (a subset of) the data as indicated in Fig. 2. We normalize the interference orders by the central value of the configuration with the most slits within a given order to remove any experiment-specific proportionality factors [13, 14, 31]. For example, for two slits A and B , we use $\bar{I}_{2,AB}^{(2)} = I_{2,AB}^{(2)}/G_{AB}^{(2)}(0,0)$, where we have explicitly indicated the involved slits. For the fifth order in two-particle correlations, this corresponds to the normalized two-particle Sorkin parameter of Eq. (5), $\kappa^{(2)} \equiv \bar{I}_5^{(2)}$.

In the intensity regime, the CCD covers the interval $\delta \in [-3\pi, +3\pi]$ of the interference pattern and thus reveals the spatial behavior of the interference orders. The results for single-particle and two-particle correlations are shown in Fig. 2(a): Solid lines correspond to experimental data and dashed lines to the quantum-mechanical theory. Single-particle interference (blue, left) vanishes starting with the third order, $\bar{I}_N^{(1)} = 0$ for $N \geq 3$, with an uncertainty of 10^{-3} , essentially limited by the relative misalignment of the slit configurations. By contrast, two-particle interference $\bar{I}_N^{(2)}$ (red, right) also exhibits a nonzero third and fourth order, while only the fifth order disappears. The modulation of the fourth-order two-particle interference [inset of Fig. 2(a)] is of the order of 10^{-1} , clearly identifiable with a good signal-to-noise ratio.

The difference between single-particle and two-particle correlations can be seen most prominently at $\delta = 0$ also in the photon-counting regime [Fig. 2(b)]. While single-particle and two-particle correlations exhibit both nonzero interference of the second order (though with

a different value due to the normalization), the difference between the two is clearly visible for the third-order term with $\bar{I}_3^{(1)} = -0.03 \pm 0.07$ being effectively zero and $\bar{I}_3^{(2)} = 0.35 \pm 0.08$ being statistically different from zero [32]. The same holds true for the interference of the fourth order with $\bar{I}_4^{(1)} = 0.03 \pm 0.04$ and $\bar{I}_4^{(2)} = 0.10 \pm 0.07$ [33]. On the other hand, the fifth-order interference is effectively zero for both single-particle and two-particle correlations.

The fifth-order term $\bar{I}_5^{(2)}$ can be used to rule out higher-order interference in two-particle correlations via the Sorkin parameter of Eq. (5). The experimental findings for $\kappa^{(2)}$ are shown in Fig. 3 for (a) intensity correlations (with statistical errors resulting from averaging over different pixels) and (b) photon correlations (with Poissonian errors), each consisting of 100 independent sets of measurements. We obtain $\kappa_{IC}^{(2)} = (-4.41 \pm 6.62) \cdot 10^{-3}$ in the intensity-correlation (IC) regime and $\kappa_{PC}^{(2)} = (-1.73 \pm 6.95) \cdot 10^{-2}$ in the photon-correlation (PC) regime.

Conclusions. We have performed a detailed experimental study of higher-order quantum interference in many-particle correlations using a two-photon-five-slit setup, both in the intensity and in the photon-counting regimes. The current experiment establishes a bound on higher-order interferences in quantum mechanics on the order of $10^{-2} - 10^{-3}$ at the level of two-particle correlations. These upper limits are of the same order of magnitude as the first experiment investigating the single-particle Sorkin parameter [9]. So far, the single-particle bounds have been lowered to $10^{-3} - 10^{-5}$ by using a more stabilized assembly [12]. An integrated photonic network scheme would even be better suited due to the relatively low losses when compared with our free-space setup. These improvements could be applied in the future also to many-particle correlations. However, due to the exponential increase of interfering quantum paths with growing particle number, the sensitivity to deviations from quantum theory by use of the many-particle Sorkin parameters of Eq. (5) is expected to be significantly higher than its single-particle counterpart: from one order of magnitude for the considered two-particle example up to 12 orders of magnitude for eight-particle correlations [29]. Since interference in eight-particle correlations has already been measured [34], many-particle interference appears to be a promising approach for high-precision tests of quantum theory.

Acknowledgments. M.-O.P. acknowledges financial support by the Studienstiftung des deutschen Volkes. M.-O.P. and J.v.Z. acknowledge funding by the Erlangen Graduate School in Advanced Optical Technologies (SAOT) by the German Research Foundation (DFG) in the framework of the German excellence initiative. We thank Dr. Irina Harder from the TDSU 1: Micro- & Nanostructuring at the Max Planck Institute for the Science of Light for producing the slit mask S1.

-
- [1] Feynman, R. P., Leighton, R. B. & Sands, M. *The Feynman Lectures on Physics, Vol. 3* (Addison-Wesley, Reading, 1965).
- [2] Peres, A. *Quantum Theory: Concepts and Methods* (Kluwer Academic Publishers, New York, 2002).
- [3] Sorkin, R. D. Quantum mechanics as quantum measure theory. *Mod. Phys. Lett. A* **09**, 3119–3127 (1994).
- [4] Born, M. Zur Quantenmechanik der Stoßvorgänge. *Z. Phys.* **37**, 863–867 (1926).
- [5] Niestegge, G. Three-slit experiments and quantum non-locality. *Found. Phys.* **43**, 805–812 (2013).
- [6] Dakić, B., Paterek, T. & Brukner, Č. Density cubes and higher-order interference theories. *New J. Phys.* **16**, 023028 (2014).
- [7] Henson, J. Bounding quantum contextuality with lack of third-order interference. *Phys. Rev. Lett.* **114**, 220403 (2015).
- [8] Zhao, Z. *et al.* Paradoxical consequences of multipath coherence: Perfect interaction-free measurements. *Phys. Rev. A* **98**, 022108 (2018).
- [9] Sinha, U., Couteau, C., Jennewein, T., Laflamme, R. & Weihs, G. Ruling out multi-order interference in quantum mechanics. *Science* **329**, 418–421 (2010).
- [10] Hickmann, J. M., Fonseca, E. J. S. & Jesus-Silva, A. J. Born’s rule and the interference of photons with orbital angular momentum by a triangular slit. *EPL* **96**, 64006 (2011).
- [11] Söllner, I. *et al.* Testing Born’s rule in quantum mechanics for three mutually exclusive events. *Found. Phys.* **42**, 742–751 (2012).
- [12] Kauten, T. *et al.* Obtaining tight bounds on higher-order interferences with a 5-path interferometer. *New J. Phys.* **19**, 033017 (2017).
- [13] Cotter, J. P. *et al.* In search of multipath interference using large molecules. *Sci. Adv.* **3**, e1602478 (2017).
- [14] Barnea, A. R., Cheshnovsky, O. & Even, U. Matter-wave diffraction approaching limits predicted by feynman path integrals for multipath interference. *Phys. Rev. A* **97**, 023601 (2018).
- [15] Park, D. K., Moussa, O. & Laflamme, R. Three path interference using nuclear magnetic resonance: a test of the consistency of Born’s rule. *New J. Phys.* **14**, 113025 (2012).
- [16] Jin, F. *et al.* Experimental test of Born’s rule by inspecting third-order quantum interference on a single spin in solids. *Phys. Rev. A* **95**, 012107 (2017).
- [17] Hong, C. K., Ou, Z. Y. & Mandel, L. Measurement of subpicosecond time intervals between two photons by interference. *Phys. Rev. Lett.* **59**, 2044–2046 (1987).
- [18] Pan, J.-W. *et al.* Multiphoton entanglement and interferometry. *Rev. Mod. Phys.* **84**, 777–838 (2012).
- [19] Tichy, M. C. Interference of identical particles from entanglement to boson-sampling. *J. Phys. B At. Mol. Opt. Phys.* **47**, 103001 (2014).
- [20] Agne, S. *et al.* Observation of genuine three-photon interference. *Phys. Rev. Lett.* **118**, 153602 (2017).
- [21] Menssen, A. J. *et al.* Distinguishability and many-particle interference. *Phys. Rev. Lett.* **118**, 153603 (2017).
- [22] Giovannetti, V., Lloyd, S. & Maccone, L. Advances in quantum metrology. *Nat. Photonics* **5**, 222–229 (2011).
- [23] Su, Z.-E. *et al.* Multiphoton interference in quantum Fourier transform circuits and applications to quantum metrology. *Phys. Rev. Lett.* **119**, 080502 (2017).
- [24] Hanbury Brown, R. & Twiss, R. Q. A test of a new type of stellar interferometer on Sirius. *Nature* **178**, 1046–1048 (1956).
- [25] Thiel, C. *et al.* Quantum imaging with incoherent photons. *Phys. Rev. Lett.* **99**, 133603 (2007).
- [26] Schneider, R. *et al.* Quantum imaging with incoherently scattered light from a free-electron laser. *Nat. Phys.* **14**, 126–129 (2018).
- [27] Aaronson, S. & Arkhipov, A. The computational complexity of linear optics. In *Proceedings of the 43rd Annual ACM Symposium on Theory of Computing, STOC ’11*, 333–342 (ACM, New York, NY, USA, 2011).
- [28] Wang, H. *et al.* Boson sampling with 20 input photons and a 60-mode interferometer in a 10^{14} -dimensional Hilbert space. *Phys. Rev. Lett.* **123**, 250503 (2019).
- [29] Pleinert, M.-O., von Zanthier, J. & Lutz, E. Many-particle interference to test Born’s rule. *Phys. Rev. Research* **2**, 012051(R) (2020).
- [30] Glauber, R. J. The quantum theory of optical coherence. *Phys. Rev.* **130**, 2529–2539 (1963).
- [31] Magaña-Loaiza, O. S. *et al.* Exotic looped trajectories of photons in three-slit interference. *Nat. Commun.* **7**, 13987 (2016).
- [32] Second- and third-order terms are a little smaller than expected, which suggests a slight off-center measurement.
- [33] Due to a difficult alignment, this result has been obtained with 100 re-measurements of only the configuration *ABCD* and its sub-configurations.
- [34] Oppel, S., Wiegner, R., Agarwal, G. S. & von Zanthier, J. Directional superradiant emission from statistically independent incoherent nonclassical and classical sources. *Phys. Rev. Lett.* **113**, 263606 (2014).